Computation of the dynamic response of finite two-dimensional periodic structures

Denis Duhamel

Computation of the dynamic response of finite two-dimensional periodic structures

Denis Duhamel

Ecole des Ponts ParisTech, Laboratoire Navier, ENPC/UGE/CNRS, 6 et 8 Avenue Blaise Pascal, Cité Descartes, Champs sur Marne, 77455 Marne la Vallée cedex 2, France

E-mail: denis.duhamel@enpc.fr

Abstract. The study of periodic media is mainly focused on one-dimensional periodic structures (periodic along one direction), to determine the dispersion curves or for the calculation of the response to an external excitation. Effective methods such as the Wave Finite Element (WFE) have been obtained for such computations. Two-dimensional periodic media are more complex to analyse but dispersion curves can be obtained rather easily. Obtaining their response to an excitation is much more difficult and the results mainly concern infinite media while for finite media, few results are available. In this communication, the response of finite two-dimensional periodic structures to an excitation is studied by limiting oneself to structures described by a scalar variable (acoustic, thermal, membrane behaviour) and having symmetries. Using the WFE for a rectangular substructure and imposing the wavenumber in one direction, we can calculate the wavenumbers and mode shapes associated with propagation in the perpendicular direction. By building solutions with null forces on parallel boundaries, we can decouple the waves in the two directions parallel to the sides of the rectangle and solve each case by a FFT. Summing the contributions of all these waves gives the global solution with a low computing time even for a large number of substructures. Examples are given for the case of a two-dimensional membrane.

1. Introduction

Authors interested in two-dimensional periodic media first aimed to determine the dispersion curves like [1] who considered wave propagation in one, two and three-dimensional periodic structures using finite element models or [2] who considered two-dimensional wave propagation in periodic lattices made of beams. More complex structures were considered by [3, 4, 5, 6] who computed dispersion relations for wave propagation in two-dimensional periodic structures by the Wave Finite Element method (WFE). Most of these authors considered a reduced model obtained by the Craig-Bampton method while in [7, 8, 9, 10] the reduction of the boundary degrees of freedom was considered in addition and [11] projected the mass and stiffness matrices on a reduced set of Bloch modes.

One can also be interested in the response of a periodic medium to an external excitation. For instance, the computation of infinite doubly periodic structures for harmonic electromagnetic fields was considered by [12] using hybrid Finite Element/Boundary Integral and periodic Green's functions. The forced response of infinite two-dimensional periodic media using WFE was computed by [13] while [14] focused on homogeneous media still using WFE but with a contour integration to improve the computation of some integrals giving the force response.

The responses of two-dimensional finite and infinite periodic structures to point harmonic and impulsive forces were also computed by [15, 16]. For finite structures, he found the solution by a modal summation of modes with periodic boundary conditions and then extended the solution to infinite structures for points far enough from the load. Experiments were also done by [17] for the seismic isolation by two-dimensional finite periodic foundations and they found interesting isolation effects for frequencies band gaps even for a small number of substructures for which comparisons with full Abaqus computations were done. In another domain, [18] computed the acoustic radiation of two-dimensional nearly periodic metamaterial plates with 6×6 substructures by the finite element method with the Craig-Bampton reduction and interpolation strategies to reduce the computational cost. In [19] two-dimensional periodic metamaterial structures were computed using interior dofs reduction by the Craig-Bampton method and an interface dofs reduction while [20] used an approximate solution built from a linear superposition of waves and computed finite two-dimensional periodic structures up to 30×30 substructures. In all cases, the number of substructures was very limited of the order of a few hundred to the maximum and the main goal was to develop reduction methods for substructures to accelerate calculations.

In this paper, we consider the calculation of a finite two-dimensional periodic medium made of a large number of substructures under external excitations. We will limit ourselves to media described by a scalar equation such as during the propagation of acoustic waves or vibrations of membranes and having symmetries with respect to two orthogonal planes parallel to the edges of a substructure. One bases on the WFE by modeling a rectangular substructure by a finite element model (FEM). By imposing the wavenumber in one direction, we can numerically calculate the wavenumbers and mode shapes associated with propagation in the perpendicular direction. By taking appropriately chosen solutions, we can decouple the waves in the two directions parallel to the sides of the rectangle. The solution of each of these two problems is obtained by a fast Fourier transformation which gives the amplitudes associated with the waves. We thus obtain the global solution for a two-dimensional periodic medium with a large number of substructures with a low computing time.

The paper is organised as follows. In section 2, wave modes for two-dimensional periodic media are computed. Special symmetric solutions are computed in section 3 and then the equations of the global problem are set and solved in section 4. Section 5 presents some numerical results for the case of a two-dimensional membrane with many substructures before the conclusion.

2. Two-dimensional wave modes

2.1. Relations on boundary variables

The discrete dynamic equation of a substructure obtained from a FE model at a circular frequency ω and for the time dependence $e^{i\omega t}$ is given by:

$$(\mathbf{K} - \omega^2 \mathbf{M})\tilde{\mathbf{q}} = \tilde{\mathbf{f}} \tag{1}$$

where $\mathbf{K}$ and $\mathbf{M}$ are the stiffness and mass matrices, respectively. $\tilde{\mathbf{f}}$ is the loading vector and $\tilde{\mathbf{q}}$ the vector of the degrees of freedom (dofs). Introducing the dynamic stiffness matrix $\widetilde{\mathbf{D}} = \mathbf{K} - \omega^2 \mathbf{M}$, decomposing the dofs into boundary (b) and interior (i) dofs, and assuming that there are no external forces on the interior nodes, result in the following equation:

$$\begin{bmatrix} \widetilde{\mathbf{D}}_{bb} & \widetilde{\mathbf{D}}_{bi} \\ \widetilde{\mathbf{D}}_{ib} & \widetilde{\mathbf{D}}_{ii} \end{bmatrix} \begin{bmatrix} \mathbf{q}_b \\ \mathbf{q}_i \end{bmatrix} = \begin{bmatrix} \mathbf{f}_b \\ \mathbf{0} \end{bmatrix} \tag{2}$$

The interior dofs can be eliminated using the second row of equation (2), which results in

$$\mathbf{q}_i = -\widetilde{\mathbf{D}}_{ii}^{-1} \widetilde{\mathbf{D}}_{ib} \mathbf{q}_b, \quad \mathbf{f}_b = \left(\widetilde{\mathbf{D}}_{bb} - \widetilde{\mathbf{D}}_{bi} \widetilde{\mathbf{D}}_{ii}^{-1} \widetilde{\mathbf{D}}_{ib} \right) \mathbf{q}_b = \mathbf{D}_b \mathbf{q}_b \tag{3}$$

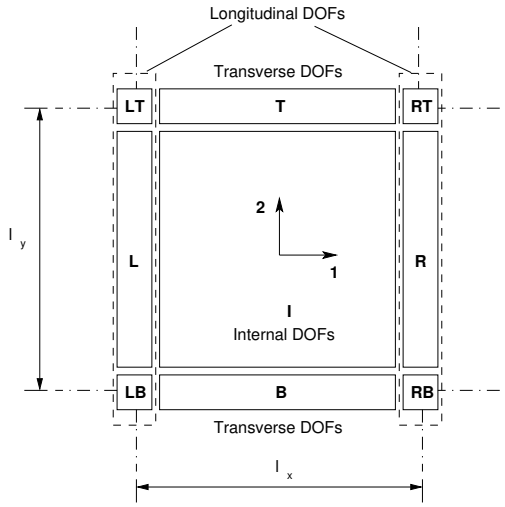

Figure 1. A substructure in the periodic medium.

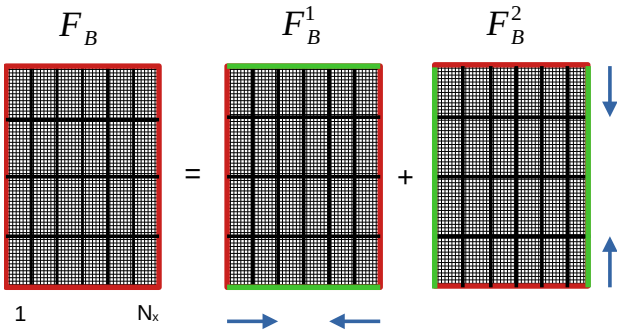

Figure 2. Decomposition of boundary loads into two side loads.

The subscript b will be dropped in the following and only boundary dofs will be considered.

2.2. Condensation of transverse degrees of freedom

The substructure is meshed with an equal number of nodes on their opposite sides. The boundary dofs are decomposed into left (L), right (R), bottom (B), top (T) dofs and associated corners (LB), (RB), (LT) and (RT) as shown in figure 1. The global vector of boundary dofs is defined as

$$\mathbf{q} = {}^t\left[\begin{array}{cccccccc} {}^t\mathbf{q}_{LB} & {}^t\mathbf{q}_{L} & {}^t\mathbf{q}_{LT} & {}^t\mathbf{q}_{RB} & {}^t\mathbf{q}_{R} & {}^t\mathbf{q}_{RT} & {}^t\mathbf{q}_{B} & {}^t\mathbf{q}_{T} \end{array}\right] \tag{4}$$

Consider waves with a given propagation constant λ_y along y. The longitudinal dofs vector is defined as $\mathbf{q}_l = {}^t\left[{}^t\mathbf{q}_{LB} \quad {}^t\mathbf{q}_{L} \quad {}^t\mathbf{q}_{LT} \quad {}^t\mathbf{q}_{RB} \quad {}^t\mathbf{q}_{R} \quad {}^t\mathbf{q}_{RT}\right]$. Thus, equation (3) is rewritten as

$$\left[\begin{array}{ccc} \mathbf{D}_{ll} & \mathbf{D}_{lB} & \mathbf{D}_{lT} \\ \mathbf{D}_{Bl} & \mathbf{D}_{BB} & \mathbf{D}_{BT} \\ \mathbf{D}_{Tl} & \mathbf{D}_{TB} & \mathbf{D}_{TT} \end{array}\right] \left[\begin{array}{c} \mathbf{q}_l \\ \mathbf{q}_B \\ \mathbf{q}_T \end{array}\right] = \left[\begin{array}{c} \mathbf{f}_l \\ \mathbf{f}_B \\ \mathbf{f}_T \end{array}\right] \tag{5}$$

Using pseudo periodic conditions with the given propagation constant λ_y and the effort equilibrium at the bottom side of the substructure, relations between the transverse dofs are given by

$$\mathbf{q}_T = \lambda_y \mathbf{q}_B, \quad \mathbf{f}_B + \frac{1}{\lambda_y}\mathbf{f}_T = 0 \tag{6}$$

Multiplying the third row of equation (5) with $\frac{1}{\lambda_y}$, taking the sum of the second and third rows of equation (5), using conditions (6), lead to

$$\mathbf{q}_B = -\left(\mathbf{D}_{BB} + \mathbf{D}_{TT} + \frac{1}{\lambda_y}\mathbf{D}_{TB} + \lambda_y \mathbf{D}_{BT}\right)^{-1}\left(\mathbf{D}_{Bl} + \frac{1}{\lambda_y}\mathbf{D}_{Tl}\right)\mathbf{q}_l \tag{7}$$

Using (6) and (7), the first row of equation (5) becomes

$$\begin{aligned} \mathbf{f}_l &= \left[\mathbf{D}_{ll} - (\mathbf{D}_{lB} + \lambda_y \mathbf{D}_{lT})\left(\mathbf{D}_{BB} + \mathbf{D}_{TT} + \frac{1}{\lambda_y}\mathbf{D}_{TB} + \lambda_y \mathbf{D}_{BT}\right)^{-1}\left(\mathbf{D}_{Bl} + \frac{1}{\lambda_y}\mathbf{D}_{Tl}\right)\right]\mathbf{q}_l \\ &= \mathbf{D}_l \mathbf{q}_l \end{aligned} \tag{8}$$

which defines the dynamic stiffness matrix $\mathbf{D}_l$ for longitudinal dofs.

2.3. One-dimensional eigenvalue problem

Using the pseudo periodic conditions also leads to these relations between longitudinal dofs

$$\begin{array}{lcl} \mathbf{q}_R &=& \lambda_x \mathbf{q}_L \\ \mathbf{q}_{RB} &=& \lambda_x \mathbf{q}_{LB} \\ \mathbf{q}_{RT} &=& \lambda_x \lambda_y \mathbf{q}_{LB} \\ \mathbf{q}_{LT} &=& \lambda_y \mathbf{q}_{LB} \end{array} \tag{9}$$

From the pseudo periodic conditions (9), it can be seen that all components of the vector $\mathbf{q}_l$ depend on the reduced set of dofs defined by $\mathbf{q}_r = {}^t\left[{}^t\mathbf{q}_{LB} \quad {}^t\mathbf{q}_L\right]$. This can be expressed as

$$\mathbf{q}_l = \left(\mathbf{W}_0(\lambda_y) + \lambda_x \mathbf{W}_1(\lambda_y)\right) \mathbf{q}_r \tag{10}$$

where the matrices $\mathbf{W}_0(\lambda_y)$ and $\mathbf{W}_1(\lambda_y)$ depend on the propagation constant λ_y and are given by

$$\mathbf{W}_0(\lambda_y) = \begin{bmatrix} \mathbf{I} & \mathbf{O} \\ \mathbf{O} & \mathbf{I} \\ \lambda_y \mathbf{I} & \mathbf{O} \\ \mathbf{O} & \mathbf{O} \\ \mathbf{O} & \mathbf{O} \\ \mathbf{O} & \mathbf{O} \end{bmatrix} \qquad \mathbf{W}_1(\lambda_y) = \begin{bmatrix} \mathbf{O} & \mathbf{O} \\ \mathbf{O} & \mathbf{O} \\ \mathbf{O} & \mathbf{O} \\ \mathbf{I} & \mathbf{O} \\ \mathbf{O} & \mathbf{I} \\ \lambda_y \mathbf{I} & \mathbf{O} \end{bmatrix} \tag{11}$$

The equilibrium conditions between adjacent substructures can be written as

$$\left(\lambda_x \mathbf{W}_0^T(\frac{1}{\lambda_y}) + \mathbf{W}_1^T(\frac{1}{\lambda_y})\right) \mathbf{f}_l = 0 \tag{12}$$

Combining (8), (10) and (12), lead to

$$\left(\lambda_x \mathbf{W}_0^T(\frac{1}{\lambda_y}) + \mathbf{W}_1^T(\frac{1}{\lambda_y})\right) \mathbf{D}_l(\lambda_y) \left(\mathbf{W}_0(\lambda_y) + \lambda_x \mathbf{W}_1(\lambda_y)\right) \mathbf{q}_r = 0 \tag{13}$$

A small damping is introduced by taking $(1+\xi i)\omega$ instead of ω with $\xi = 0.0001$. So we always have $|\lambda_x| \neq 1$ and the right-going solutions must have a decreasing amplitude as we move on the right, meaning that

$$|\lambda_x| < 1, \quad |\lambda_x^\star| > 1 \tag{14}$$

This allows to define the two sets of eigensolutions

$$\begin{array}{rcl} \mathbf{\Lambda}(\lambda_y) & = [\lambda_{\mathtt{x}1}(\lambda_y) \cdots \lambda_{\mathtt{x}n}(\lambda_y)] & , \quad \mathbf{\Lambda}^\star(\lambda_y) = [\lambda^\star_{\mathtt{x}1}(\lambda_y) \cdots \lambda^\star_{\mathtt{x}n}(\lambda_y)] \\ \mathbf{\Phi}_{\mathtt{q}}(\lambda_y) & = [\boldsymbol{\phi}_{\mathtt{q}1}(\lambda_y) \cdots \boldsymbol{\phi}_{\mathtt{q}n}(\lambda_y)] & , \quad \mathbf{\Phi}^\star_{\mathtt{q}}(\lambda_y) = [\boldsymbol{\phi}^\star_{\mathtt{q}1}(\lambda_y) \cdots \boldsymbol{\phi}^\star_{\mathtt{q}n}(\lambda_y)] \\ \mathbf{\Phi}_{\mathtt{F}}(\lambda_y) & = [\boldsymbol{\phi}_{\mathtt{F}1}(\lambda_y) \cdots \boldsymbol{\phi}_{\mathtt{F}n}(\lambda_y)] & , \quad \mathbf{\Phi}^\star_{\mathtt{F}}(\lambda_y) = [\boldsymbol{\phi}^\star_{\mathtt{F}1}(\lambda_y) \cdots \boldsymbol{\phi}^\star_{\mathtt{F}n}(\lambda_y)]. \end{array} \tag{15}$$

in which $\boldsymbol{\phi}_{\mathtt{qj}}$ is the solution of the eigenproblem (13) and $\boldsymbol{\phi}_{\mathtt{Fj}} = {}^t\left[{}^t\mathbf{f}^j_{LB} \quad {}^t\mathbf{f}^j_L\right]$ the associated force vector.

3. Building eigenvectors with free boundary

3.1. Reduction to one-dimensional problems

Consider now a rectangular domain which undergoes forces over its left/right and bottom/top edges, as depicted in Figure 2 where the loads are shown as red lines on the boundary while free sides are depicted as green lines. The global loads can be decomposed as loads on the vertical

sides $\mathbf{F}_B^1$ and loads on the horizontal sides $\mathbf{F}_B^2$ such that the displacements of the global problem can be recovered as the sum of the displacements of problems 1 and 2. So we have

$$\mathbf{F}_B = (\mathbf{F}_B)^1 + (\mathbf{F}_B)^2 \quad \Rightarrow \quad \mathbf{q}_B = (\mathbf{q}_B)^1 + (\mathbf{q}_B)^2. \tag{16}$$

We focus now on one of the two problems defined previously. Consider for instance the first problem as the second problem can be solved in the same way. From the knowledge of the propagation constants and wave modes for one-dimensional WFE, the vectors of displacements and forces of an assembly of N_x substructures like the one displayed in Figure 2 are expressed on global left and right boundaries in terms of wave shapes, as follows:

$$\begin{aligned} \mathbf{q}_L &= \mathbf{\Phi}_{\mathtt{q}}\mathbf{Q} + \mathbf{\Phi}_{\mathtt{q}}^{\star}\boldsymbol{\mu}^{N_x}\mathbf{Q}^{\star}, \quad -\mathbf{F}_L &= \mathbf{\Phi}_{\mathtt{F}}\mathbf{Q} + \mathbf{\Phi}_{\mathtt{F}}^{\star}\boldsymbol{\mu}^{N_x}\mathbf{Q}^{\star} \\ \mathbf{q}_R &= \mathbf{\Phi}_{\mathtt{q}}\boldsymbol{\mu}^{N_x}\mathbf{Q} + \mathbf{\Phi}_{\mathtt{q}}^{\star}\mathbf{Q}^{\star}, \quad \mathbf{F}_R &= \mathbf{\Phi}_{\mathtt{F}}\boldsymbol{\mu}^{N_x}\mathbf{Q} + \mathbf{\Phi}_{\mathtt{F}}^{\star}\mathbf{Q}^{\star} \end{aligned} \tag{17}$$

where $\mathbf{Q}$ and $\mathbf{Q}^{\star}$ are vectors of wave amplitudes which are respectively defined at the left and right edges of the whole domain. The elements of the diagonal matrix $\boldsymbol{\mu}$ have modulus less or equal to one. The main problem is to find the wave modes $\mathbf{\Phi}_{\mathtt{F}}$ and $\mathbf{\Phi}_{\mathtt{F}}^{\star}$ with free boundaries (no force on the bottom and top boundaries).

3.2. Symmetric solution

We suppose now that the geometry and the mechanical parameters of a period are invariant by substituting $l_y - y$ to y. Consider a solution defined by the vectors

$$\begin{bmatrix} \mathbf{q}_l \\ \mathbf{q}_B \\ \mathbf{q}_T \end{bmatrix} \quad and \quad \begin{bmatrix} \mathbf{f}_l \\ \mathbf{f}_B \\ \mathbf{f}_T \end{bmatrix} \tag{18}$$

Now, denoting $\mathbf{q}(x, y)$ the displacement associated to this solution, one defines the symmetric solution such that

$$\tilde{\mathbf{q}}(x, y) = \frac{1}{\lambda_y}\mathbf{q}(x, l_y - y) \tag{19}$$

So the symmetric solution is such that

$$\tilde{\mathbf{q}}_B = \mathbf{q}_B, \quad and \quad \tilde{\mathbf{q}}_T = \frac{1}{\lambda_y}\tilde{\mathbf{q}}_B = \frac{1}{\lambda_y}\mathbf{q}_B \tag{20}$$

Concerning the forces, one has

$$\begin{aligned} \tilde{\mathbf{f}}_B &= \mathbf{D}_{Bl}\tilde{\mathbf{q}}_l + \mathbf{D}_{BB}\tilde{\mathbf{q}}_B + \mathbf{D}_{BT}\tilde{\mathbf{q}}_T \\ \tilde{\mathbf{f}}_T &= \mathbf{D}_{Tl}\tilde{\mathbf{q}}_l + \mathbf{D}_{TB}\tilde{\mathbf{q}}_B + \mathbf{D}_{TT}\tilde{\mathbf{q}}_T \end{aligned} \tag{21}$$

We make the hypothesis that the symmetry of the structure leads to the following relations on the submatrices.

$$\mathbf{D}_{BB} = \mathbf{D}_{TT}, \quad \mathbf{D}_{BT} = \mathbf{D}_{TB}, \quad \mathbf{D}_{TB} = \mathbf{D}_{BT} \tag{22}$$

From this, one can prove that the symmetric solution satisfies

$$\tilde{\mathbf{f}}_B = -\mathbf{f}_B, \quad \tilde{\mathbf{f}}_T = -\frac{1}{\lambda_y}\tilde{\mathbf{f}}_B \tag{23}$$

This shows that the symmetric solution is associated to the propagation constant $\frac{1}{\lambda_y}$. One can also check that

$$\left(\lambda_x \mathbf{W}_0^T(\lambda_y) + \mathbf{W}_1^T(\lambda_y)\right) \mathbf{D}_l(\frac{1}{\lambda_y}) \left(\mathbf{W}_0(\frac{1}{\lambda_y}) + \lambda_x \mathbf{W}_1(\frac{1}{\lambda_y})\right) \tilde{\mathbf{q}}_r = 0 \tag{24}$$

and $\tilde{\mathbf{q}}_r$ is associated to the propagation constant λ_x in the x direction and to $\frac{1}{\lambda_y}$ in the y direction.

4. Fast solution for the two-dimensional periodic structures

4.1. Decomposition of force vectors

The solution is searched under the form of waves associated to propagation constants $\lambda_{y,n} = e^{i\pi n/N_y}$ along y, for $-N_y \leq n \leq N_y - 1$, leading to the propagation constants λ^{x+} and λ^{x-} along x. Along x one has propagation constants $\lambda_{x,m} = e^{i\pi m/N_x}$, for $-N_x \leq m \leq N_x - 1$, leading to the propagation constants λ^{y+} and λ^{y-} along y. For instance, the force on the global bottom boundary can then be decomposed as

$$\begin{aligned}\mathbf{f}_B(p_B) &= \sum_{n=-N_y}^{n=N_y-1} \left(\mathbf{F}_{Bn}^{x+}(\mathbf{\Lambda}_n^{x+})^{p_B}\mathbf{a}_n^{x+} + \mathbf{F}_{Bn}^{x-}(\mathbf{\Lambda}_n^{x-})^{p_B-(N_x-1)}\mathbf{a}_n^{x-}\right) \\ &+ \sum_{m=-N_x}^{m=N_x-1} e^{i\pi p_B m/N_x}\left(\mathbf{F}_{Bm}^{y+}\mathbf{a}_m^{y+} + \mathbf{F}_{Bm}^{y-}(\mathbf{\Lambda}_m^{y-})^{-(N_y-1)}\mathbf{a}_m^{y-}\right)\end{aligned} \tag{25}$$

for $0 \leq p_B \leq N_x - 1$ and where $|\lambda_{nj}^{x+}|, |\lambda_{nj}^{y+}| < 1$, $|\lambda_{nj}^{x-}|, |\lambda_{nj}^{y-}| > 1$ and for instance

$$\begin{aligned}\mathbf{\Lambda}_n^{x+} &= diag\left(\lambda_{nj}^{x+}\right)_{j=1\ldots J_n^+}, & \mathbf{\Lambda}_n^{x-} &= diag\left(\lambda_{nj}^{x-}\right)_{j=1\ldots J_n^-} \\ \mathbf{F}_{Xn}^{x+} &= \left[\mathbf{f}_{Xn1}^{x+}, ..., \mathbf{f}_{Xnj}^{x+}, ..., \mathbf{f}_{XnJ_n^+}^{x+}\right], & \mathbf{F}_{Xn}^{x-} &= \left[\mathbf{f}_{Xn1}^{x-}, ..., \mathbf{f}_{Xnj}^{x-}..., \mathbf{f}_{XnJ_n^-}^{x-}\right] \\ \mathbf{a}_n^{x+} &= \left[a_{n1}^{x+}, ..., a_{nj}^{x+}, ..., a_{nJ_n^+}^{x+}\right]^T, & \mathbf{a}_n^{x-} &= \left[a_{n1}^{x-}, ..., a_{nj}^{x-}, ..., a_{nJ_n^-}^{x-}\right]^T\end{aligned} \tag{26}$$

From relations (13), one has in a general way,

$$\mathbf{\Lambda}_n^{x+} = (\mathbf{\Lambda}_{-n}^{x-})^{-1}, \quad \mathbf{\Lambda}_m^{y+} = (\mathbf{\Lambda}_{-m}^{y-})^{-1} \tag{27}$$

Supposing that the substructure is symmetric, we also have

$$\begin{aligned}\mathbf{\Lambda}_{-n}^{x+} &= \mathbf{\Lambda}_n^{x+}, \;\; \mathbf{\Lambda}_{-n}^{x-} = \mathbf{\Lambda}_{-n}^{x-}, \;\; \mathbf{\Lambda}_{-n}^{y+} = \mathbf{\Lambda}_n^{y+}, \;\; \mathbf{\Lambda}_n^{y-} = \mathbf{\Lambda}_{-n}^{y-} \\ \mathbf{F}_{B(-n)}^{x+} &= -\mathbf{F}_{Bn}^{x+}, \;\; \mathbf{F}_{B(-n)}^{x-} = -\mathbf{F}_{Bn}^{x-}\end{aligned} \tag{28}$$

One can choose the decomposition such that

$$\mathbf{a}_{-n}^{x+} = \mathbf{a}_n^{x+}, \;\; \mathbf{a}_{-n}^{x-} = \mathbf{a}_n^{x-}, \;\; \mathbf{a}_{-m}^{y+} = \mathbf{a}_m^{y+}, \;\; \mathbf{a}_{-m}^{y-} = \mathbf{a}_m^{y-} \tag{29}$$

Inserting relations (27), (28) and (29) into (25) leads to

$$\mathbf{f}_B(p_B) = \sum_{m=-N_x}^{m=N_x-1} e^{i\pi p_B m/N_x}\left(\mathbf{F}_{Bm}^{y+}\mathbf{a}_m^{y+} + \mathbf{F}_{Bm}^{y-}(\mathbf{\Lambda}_m^{y-})^{-(N_y-1)}\mathbf{a}_m^{y-}\right)$$

Using the relation

$$\mathbf{F}_{Tm}^{y-} + \mathbf{F}_{Bm}^{y-}\mathbf{\Lambda}_m^{y-} = 0 \tag{30}$$

we finally get

$$\mathbf{f}_B(p_B) = \sum_{m=-N_x}^{m=N_x-1} e^{i\pi p_B m/N_x}\left(\mathbf{F}_{Bm}^{y+}\mathbf{a}_m^{y+} - \mathbf{F}_{Tm}^{y-}(\mathbf{\Lambda}_m^{y-})^{-N_y}\mathbf{a}_m^{y-}\right) \tag{31}$$

And similar relations for the three other parts of the boundary.

4.2. System to solve
The precedent relations can be written in a more compact form as

$$\begin{aligned}
\mathbf{F}_B &= \boldsymbol{\omega}_x \mathbf{F}_B^{y+} \mathbf{a}^{y+} - \boldsymbol{\omega}_x \mathbf{F}_T^{y-} (\boldsymbol{\Lambda}^{y-})^{-N_y} \mathbf{a}^{y-} \\
\mathbf{F}_R &= -\boldsymbol{\omega}_y \mathbf{F}_L^{x+} (\boldsymbol{\Lambda}^{x+})^{N_x} \mathbf{a}^{x+} + \boldsymbol{\omega}_y \mathbf{F}_R^{x-} \mathbf{a}^{x-} \\
\mathbf{F}_T &= -\boldsymbol{\omega}_x \mathbf{F}_B^{y+} (\boldsymbol{\Lambda}^{y+})^{N_y} \mathbf{a}^{y+} + \boldsymbol{\omega}_x \mathbf{F}_T^{y-} \mathbf{a}^{y-} \\
\mathbf{F}_L &= \boldsymbol{\omega}_y \mathbf{F}_L^{x+} \mathbf{a}^{x+} - \boldsymbol{\omega}_y \mathbf{F}_R^{x-} (\boldsymbol{\Lambda}^{x-})^{-N_x} \mathbf{a}^{x-}
\end{aligned} \tag{32}$$

with for instance

$$\begin{aligned}
\mathbf{F}_L &= \begin{pmatrix} \mathbf{f}_L(0) \\ \mathbf{f}_L(1) \\ \vdots \\ \mathbf{f}_L(N_y-1) \end{pmatrix} \\
\mathbf{F}_L^{x+} &= diag\left(\mathbf{F}_{L(-N_y)}^{x+}, ..., \mathbf{F}_{Ln}^{x+}, ..., \mathbf{F}_{LN_y-1}^{x+}\right), \quad \mathbf{F}_L^{x-} = diag\left(\mathbf{F}_{R(-N_y)}^{x-}, ..., \mathbf{F}_{Rn}^{x-}, ..., \mathbf{F}_{RN_y-1}^{x-}\right) \\
\boldsymbol{\Lambda}^{x-} &= diag\left(\boldsymbol{\Lambda}_{-N_y}^{x-}, ..., \boldsymbol{\Lambda}_{n}^{x-}, ..., \boldsymbol{\Lambda}_{N_y-1}^{x-}\right), \quad \boldsymbol{\omega}_y = \left(\lambda_y^{nm} \mathbf{I}_{nm}\right)_{0 \le n \le N_y-1, -N_y \le m \le N_y-1}
\end{aligned} \tag{33}$$

with $\lambda_y = e^{i\pi/N_y}$, $\mathbf{I}_{nm} = \mathbf{I}_{n_l \times n_l}$ and $n_l = n_{LB} + n_L$ the number of reduced dofs.

4.3. Symmetric relations
Consider relation (31), one has

$$\begin{aligned}
\mathbf{f}_B(p_B) &= \sum_{m=-N_x}^{m=N_x-1} e^{i\pi p_B m/N_x} \left(\mathbf{F}_{Bm}^{y+} \mathbf{a}_m^{y+} - \mathbf{F}_{Tm}^{y-} (\boldsymbol{\Lambda}_m^{y-})^{-N_y} \mathbf{a}_m^{y-}\right) \\
&= \sum_{m=-N_x}^{m=N_x-1} e^{-i\pi p_B m/N_x} \left(\mathbf{F}_{B(-m)}^{y+} \mathbf{a}_m^{y+} - \mathbf{F}_{T(-m)}^{y-} (\boldsymbol{\Lambda}_m^{y-})^{-N_y} \mathbf{a}_m^{y-}\right)
\end{aligned} \tag{34}$$

because $\lambda_{x,-N_x} = \lambda_{x,N_x} = -1$, and for instance $\mathbf{F}_{B(-N_x)}^{y+} = \mathbf{F}_{BN_x}^{y+}$. Note also that, for instance, $\mathbf{F}_{B(-m)}^{y+} = \frac{1}{\lambda_{x,m}} \tilde{\mathbf{F}}_{B(m)}^{y+}$, and a similar relation for the top component, so that we finally gets

$$\tilde{\mathbf{f}}_B(p_B) = \sum_{m=-N_x}^{m=N_x-1} e^{-i\pi(p_B+1)m/N_x} \left(\mathbf{F}_{Bm}^{y+} \mathbf{a}_m^{y+} - \mathbf{F}_{Tm}^{y-} (\boldsymbol{\Lambda}_m^{y-})^{-N_y} \mathbf{a}_m^{y-}\right)$$

with $\tilde{\mathbf{f}}_B(p_B)$ obtained from $\mathbf{f}_B(p_B)$ by inverting the dofs on the bottom boundary on each substructure between 0 and l_x. The function $\mathbf{f}_B(p_B)$ can now be defined for $-N_x \le p_B \le N_x - 1$ with $\mathbf{f}_B(-p_B - 1) = \tilde{\mathbf{f}}_B(p_B)$. The global system to solve is then

$$\begin{pmatrix} \mathbf{F}_B \\ \tilde{\mathbf{F}}_B \\ \mathbf{F}_R \\ \tilde{\mathbf{F}}_R \\ \mathbf{F}_T \\ \tilde{\mathbf{F}}_T \\ \mathbf{F}_L \\ \tilde{\mathbf{F}}_L \end{pmatrix} = \begin{pmatrix} \mathbf{O} & \mathbf{O} & \boldsymbol{\omega}_x^+ \mathbf{F}_B^{y+} & -\boldsymbol{\omega}_x^+ \mathbf{F}_T^{y-} (\boldsymbol{\Lambda}^{y-})^{-N_y} \\ \mathbf{O} & \mathbf{O} & \boldsymbol{\omega}_x^- \mathbf{F}_B^{y+} & -\boldsymbol{\omega}_x^- \mathbf{F}_T^{y-} (\boldsymbol{\Lambda}^{y-})^{-N_y} \\ -\boldsymbol{\omega}_y^+ \mathbf{F}_L^{x+} (\boldsymbol{\Lambda}^{x+})^{N_x} & \boldsymbol{\omega}_y^+ \mathbf{F}_R^{x-} & \mathbf{O} & \mathbf{O} \\ -\boldsymbol{\omega}_y^- \mathbf{F}_L^{x+} (\boldsymbol{\Lambda}^{x+})^{N_x} & \boldsymbol{\omega}_y^- \mathbf{F}_R^{x-} & \mathbf{O} & \mathbf{O} \\ \mathbf{O} & \mathbf{O} & -\boldsymbol{\omega}_x^+ \mathbf{F}_B^{y+} (\boldsymbol{\Lambda}^{y+})^{N_y} & \boldsymbol{\omega}_x^+ \mathbf{F}_T^{y-} \\ \mathbf{O} & \mathbf{O} & -\boldsymbol{\omega}_x^- \mathbf{F}_B^{y+} (\boldsymbol{\Lambda}^{y+})^{N_y} & \boldsymbol{\omega}_x^- \mathbf{F}_T^{y-} \\ \boldsymbol{\omega}_y^+ \mathbf{F}_L^{x+} & -\boldsymbol{\omega}_y^+ \mathbf{F}_R^{x-} (\boldsymbol{\Lambda}^{x-})^{-N_x} & \mathbf{O} & \mathbf{O} \\ \boldsymbol{\omega}_y^- \mathbf{F}_L^{x+} & -\boldsymbol{\omega}_y^- \mathbf{F}_R^{x-} (\boldsymbol{\Lambda}^{x-})^{-N_x} & \mathbf{O} & \mathbf{O} \end{pmatrix} \begin{pmatrix} \mathbf{a}^{x+} \\ \mathbf{a}^{x-} \\ \mathbf{a}^{y+} \\ \mathbf{a}^{y-} \end{pmatrix} \tag{35}$$

with

$$\tilde{\mathbf{F}}_B = \begin{pmatrix} \tilde{\mathbf{F}}_B(N_x-1) \\ \vdots \\ \tilde{\mathbf{F}}_B(0) \end{pmatrix}, \quad \mathbf{F}_B = \begin{pmatrix} \mathbf{F}_B(0) \\ \vdots \\ \mathbf{F}_B(N_x-1) \end{pmatrix}$$

$$\boldsymbol{\omega}_x^- = \begin{pmatrix} e^{-i\pi N_x m/N_x} \\ e^{-i\pi(N_x-1)m/N_x} \\ \vdots \\ e^{-i2\pi m/N_x} \\ e^{-i\pi m/N_x} \end{pmatrix}_{-N_x \le m \le N_x-1}, \quad \boldsymbol{\omega}_x^+ = \begin{pmatrix} 1 \\ e^{i\pi m/N_x} \\ \vdots \\ e^{i\pi(N_x-2)m/N_x} \\ e^{i\pi(N_x-1)m/N_x} \end{pmatrix}_{-N_x \le m \le N_x-1} \tag{36}$$

4.4. Use of FFT for an efficient solution

Taking the Fast Fourier Transform of both sides of (35) for each of the four parts of the boundary, noting that $FFT\begin{pmatrix}\boldsymbol{\omega}_x^+ \\ \boldsymbol{\omega}_x^-\end{pmatrix} = 2N_x\mathbf{I}$ and that after the FFT the right hand side is made of block matrices, the system can be decomposed as the following subsystems for each component of the FFT

$$\begin{pmatrix}\mathcal{F}_{Rn} \\ \mathcal{F}_{Ln}\end{pmatrix} = 2N_x \begin{pmatrix} -\mathbf{F}_{Ln}^{x+}(\boldsymbol{\Lambda}_n^{x+})^{N_x} & \mathbf{F}_{Rn}^{x-} \\ \mathbf{F}_{Ln}^{x+} & -\mathbf{F}_{Rn}^{x-}(\boldsymbol{\Lambda}_n^{x-})^{-N_x} \end{pmatrix} \begin{pmatrix}\mathbf{a}_n^{x+} \\ \mathbf{a}_n^{x-}\end{pmatrix} \tag{37}$$

with for instance $\mathcal{F}_{Rn}$ the n^{th} component of $fft\begin{pmatrix}\mathbf{F}_R \\ \tilde{\mathbf{F}}_R\end{pmatrix}$. The solution of this small size system gives to n^{th} component of the amplitude and the whole solution can then be rebuilt.

5. Numerical results

5.1. Validation with a homogeneous structure

We first consider the case of the Helmholtz equation (modelling acoustic or a membrane vibration) on a homogeneous medium divided into rectangular substructures. The equation is

$$\Delta p + k^2 p = 0 \ \ in \ \ \Omega, \quad \frac{\partial p}{\partial n} = q_0 \ \ over \ \partial\Omega \tag{38}$$

with $k = \omega/c$, ω the circular frequency and $c = 343m/s$ the sound velocity. The structure Ω is divided into $N_x \times N_y$ substructures of size $L_x \times L_y$. q_0 is a given function on the boundary. In this case it is simple to find an analytical solution to estimate the accuracy of the proposed method. For example a solution is $p_0(\mathbf{x}) = \frac{i}{4}H_0(k|\mathbf{x}-\mathbf{x}_s|)$ for a point source $\mathbf{x}_s$ outside the domain Ω and $q_0 = \frac{\partial}{\partial n}p_0$. We compare the results of the analytical solution, a full Finite Element (FEM) solution and the present two-dimensional WFE method in table 1 for structures with 5×5 and 25×25 substructures. The substructures are meshed with 10×10 quadratic 8 nodes elements. The sizes are $L_x = L_y = 0.1m$. The position of the source is at $\mathbf{x}_s = (-0.5m, -0.5m)$. It can be observed in table 1 that there is a perfect agreement for low frequencies and that for high frequencies the accuracy of the 2D WFE is similar to the full FEM.

5.2. Structure with holes

We consider now a substructure with a central hole of radius $0.02m$ as in figure 3. All the other properties are the same as before. The mesh of a substructure is shown in figure 3 and is made of 654 nodes with linear triangular elements obtained from gmsh. The boundary condition

Table 1. Comparison of the solution for different methods, number of substructures, frequencies and computation points.

	5×5			25×25		
100Hz	Analytic	WFE 2D	FEM	Analytic	WFE 2D	FEM
$(0,0)$	$-0.071+0.156i$	$-0.071+0.156i$	$-0.071+0.156i$	$-0.071+0.156i$	$-0.071+0.156i$	$-0.071+0.156i$
(L_x, L_y)	$-0.101+0.120i$	$-0.101+0.120i$	$-0.101+0.120i$	$-0.101+0.120i$	$-0.101+0.120i$	$-0.101+0.120i$
$(5L_x, 5L_y)$	$-0.121-0.023i$	$-0.121-0.023i$	$-0.121-0.023i$	$-0.121-0.023i$	$-0.121-0.023i$	$-0.121-0.023i$
4000Hz	Analytic	WFE 2D	FEM	Analytic	WFE 2D	FEM
$(0,0)$	$-0.019+0.020i$	$-0.021-0.002i$	$-0.014+0.016i$	$-0.019+0.020i$	$-0.023+0.020i$	$-0.021+0.019i$
(L_x, L_y)	$0.025+0.003i$	$0.026+0.022i$	$0.021+0.006i$	$0.025+0.003i$	$0.026+0.004i$	$0.025+0.004i$
$(5L_x, 5L_y)$	$-0.014-0.013i$	$-0.016-0.039i$	$-0.009-0.017i$	$-0.014-0.013i$	$-0.012-0.016i$	$-0.012-0.015i$

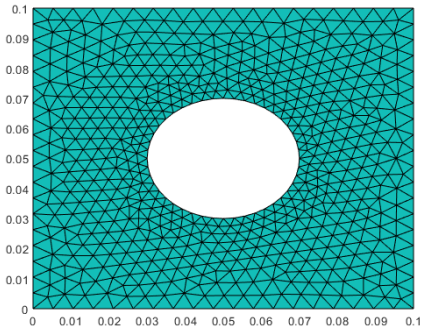

Figure 3. Substructure with a central hole.

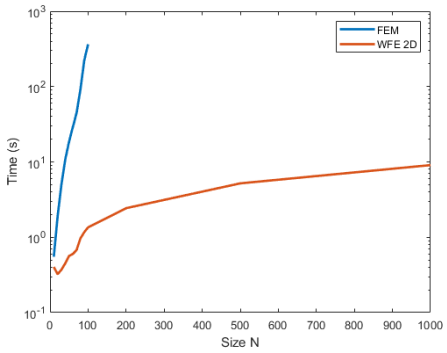

Figure 4. Computing times.

is obtained by the normal derivative of a plane wave of direction $(1/\sqrt{2}, 1/\sqrt{2})$. The case of a structure made of 25×25 substructures computed at 1000Hz is shown in figure 5 for the full FEM computation and in figure 6 for the 2D WFE. A perfect agreement between the two computations is observed. The same computation is also made for structures of increasing sizes between $N \times N = 10 \times 10$ substructures and $N \times N = 1000 \times 1000$. The computing time is shown in figure 4 for the 2D WFE. For the FEM the computation is only done up to 100×100 substructures. The computing time is strongly increasing for the FEM while it increases only mildly for the 2D WFE. Note that for the 1000×1000 structure the number of nodes for a classical FEM computation would be about 650 millions. This problem is solved by the present 2D WFE in 9 seconds with Matlab on a personal computer with a memory of 16Go and a processor Intel Core(TM) i7-9700.

6. Conclusion

We have developed a new method to compute two-dimensional periodic media for the case of a scalar wave equation. This is based on the Wave Finite Element Method by considering propagation along the two directions parallel to the boundary of a substructure. For a boundary excitation the method proves to be very efficient and allows to get the solution for structures made of millions of substructures. Future works should try to extend the method for the case of two-dimensional elasticity meaning structures described by vectorial equations and substructures having no special symmetry. The case of loading on the internal dofs should also be considered.

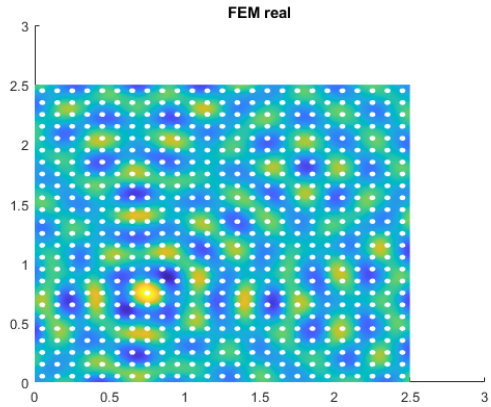

Figure 5. FEM solution at 1000z.

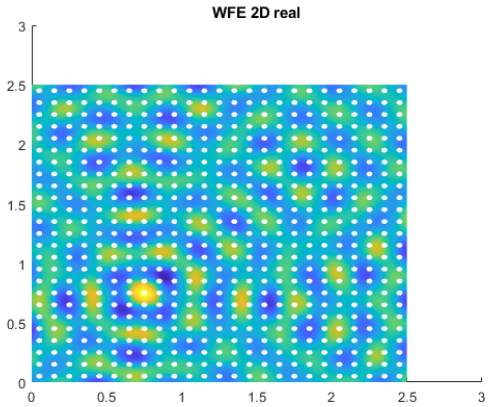

Figure 6. 2D WFE at 1000Hz.

References

[1] Abdel-Rahman A 1979 *Matrix analysis of wave propagation in periodic systems* Ph.D. thesis University of Southampton

[2] Phani A S, Woodhouse J and Fleck N A 2006 *The Journal of the Acoustical Society of America* **119** 1995–2005

[3] Manconi E 2008 *Modelling wave propagation in two–dimensional structures using a wave/finite element technique* Ph.D. thesis University of Parma

[4] Zhou C, Lainé J P, Ichchou M and Zine A 13-17 July, 2014 *21st International Congress on Sound and Vibration* (Beijing, China) pp 389–395

[5] Zhou C W, Lainé J P, Ichchou M N and Zine A M 2015 *Computers & Structures* **154** 145–162

[6] Palermo A and Marzani A 2016 *International Journal of Solids and Structures* **100-101** 29–40

[7] Krattiger D and Hussein M I 2014 *Phys. Rev. E* **90**(6) 063306

[8] Droz C, Zhou C, Ichchou M N and Lainé J P 2016 *Journal of Sound and Vibration* **363** 285–302

[9] Krattiger D and Hussein M I 2018 *Journal of Computational Physics* **357** 183–205

[10] Van Belle L, de Melo Filho N G R, Clasing Villanueva M, Claeys C, Deckers E, Naets F and Desmet W 7-9 September, 2020 *International Conference on Noise and Vibration Engineering (ISMA 2020)* (Leuven, Belgium) pp 2487–2502

[11] Hussein M I 2009 *Proc. R. Soc. A.* **465**(6) 2825–2848

[12] Eibert T F, Volakis J L, Wilton D R and Jackson D R 1999 *IEEE Transactions on Antennas and Propagation* **47** 843–850

[13] Duhamel D 2007 *Engineering Analysis with Boundary Elements* **31** 919–930

[14] Renno J M and Mace B R 2011 *Journal of Sound and Vibration* **330** 5913–5927

[15] Langley R S 1996 *Journal of Sound and Vibration* **197** 447–469

[16] Langley R S 1997 *Journal of Sound and Vibration* **201** 235–253

[17] Yan Y, Laskar A, Cheng Z, Menq F, Tang Y, Mo Y L and Shi Z 2014 *Journal of Applied Physics* **116** 044908

[18] Mencik J M and Gobert M L 12-14 Sep, 2022 *International Conference on Noise and Vibration Engineering (ISMA 2022)* (Leuven, Belgium) pp 3013–3022

[19] Van Belle L, Claeys C, Deckers E and Desmet W 25-27 October, 2021 *Proceedings of Euronoise* (Madeira, Portugal) pp 1–10

[20] Qu F, Van Belle L and Deckers E 12-14 Sep, 2022 *International Conference on Noise and Vibration Engineering (ISMA 2022)* (Leuven, Belgium) pp 3133–3147